Use of Smartphones in Optical Experimentation

Use of Smartphones in Optical Experimentation

Yiping Zhao
Yoong Sheng Phang

Tutorial Texts in Optical Engineering
Volume TT124

SPIE PRESS
Bellingham, Washington USA

Library of Congress Cataloging-in-Publication Data

Names: Zhao, Yiping, author. | Phang, Yoong Sheng, author.
Title: Use of smartphones in optical experimentation / Yiping Zhao, Yoong Sheng Phang.
Description: Bellingham, Washington, USA : SPIE Press, [2022] | Includes bibliographical references.
Identifiers: LCCN 2022023950 | ISBN 9781510654976 (paperback) | ISBN 9781510654983 (pdf)
Subjects: LCSH: Optics–Experiments. | Smartphones–Scientific applications.
Classification: LCC QC365 .Z43 2022 | DDC 535.078–dc23 /eng20220826
LC record available at https://lccn.loc.gov/2022023950

Published by

SPIE
P.O. Box 10
Bellingham, Washington 98227-0010 USA
Phone: +1 360.676.3290
Fax: +1 360.647.1445
Email: books@spie.org
Web: http://spie.org

Printed in the United States of America.
First printing 2022.
For updates to this book, visit http://spie.org and type “TT124” in the search field.

Contents

Chapter 1
Smartphones and Their Optical Sensors

1.1 History and Current Utilization in Education

A smartphone is a handheld device that integrates the basic functions of a mobile phone with advanced computing capabilities. The concept of combining a telephone and a computer chip dates to the early 1970s when Motorola introduced the first handheld cellular mobile phones. However, these cell phones were hardly ergonomic and ran on low data rate networks at speeds of less than 100 Kb/s [1]. In 1994, the Simon Personal Communicator, which is widely regarded as the world's first smartphone, was launched by IBM [2]. The Simon was the first phone to incorporate the functions of a cell phone with those of a personal digital assistant (PDA), allowing users to call, page, and fax from their cell phones [3]. The Simon was also the first to use a touchscreen and stylus and include other new features such as an address book, a calendar, a calculator, and an appointment scheduler. Access to the mobile web was introduced by the Nokia 9000 Communicator launched in 1996 [4]. In 2000, the first mobile phone camera was unveiled in Sharp's J-SH04 model, which had a 0.3-megapixel (MP) resolution and allowed users to send images electronically. The deployment of 3G networks in 2001 resulted in bit rates that were high enough to accommodate the sending and receiving of photographs, video clips, and other media [5]. It was not until the launch of Apple's iPhone in 2007 that the standards were set for the modern smartphone. For this reason, the history of smartphones has been classified into the pre-iPhone era (before 2007) and the post-iPhone era (after 2007) [6]. The iPhone brought hardware and sensors such as the accelerometer and the capacitive touchscreen into the mainstream, creating an interactive experience for the user [7]. Its iOS operating system also revolutionized internet applications on smartphones, introducing a high degree of portable accessibility and storage, and making them comparable to operating systems that run on a personal computer [8]. A year later in 2008, Google acquired Android, an open-source operating system, and licensed it to all handset

smartphone/tablet hardware and interfaces to create point-of-care diagnostic tools or portable medical devices [18]. For example, smartphones have been integrated into powerful microscopes for image analysis, colorimetric detection, blood testing, and disease diagnostics [19–30]. In combination with nanotechnology, smartphones have also been modified for use as spectrometers for chemical and biological sensing [31]. Many do-it-yourself (DIY) enthusiast websites have also demonstrated the use of smartphones/tablets in electronics projects [32]. It is evident that besides using the communication and software capabilities of smartphones/tablets for conventional m-learning, their opto-electronic/MEMS-sensing capabilities can be exploited to build laboratory instruments for hands-on lab education.

1.2 Smartphone Camera

The most important smartphone component for the experimental applications in this book is its camera. The smartphone camera usually consists of two parts: the optical sensor array and the adaptive optical system, as shown in Fig. 1.1.

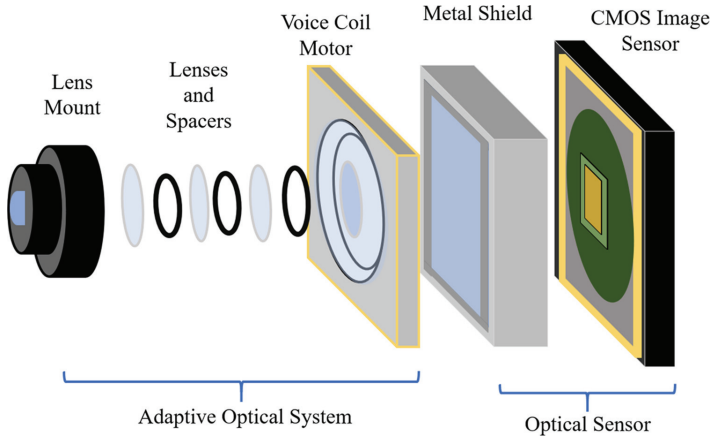

Figure 1.1 Parts of a smartphone camera system.

1.2.1 Optical sensor

The standard optical sensor used in smartphones is an active-pixel sensor called the complementary metal oxide semiconductor (CMOS). A CMOS sensor array is a silicon-based integrated circuit consisting of a two-dimensional (2D) grid of light-sensitive elements called photosites, as shown in Fig. 1.2. Each CMOS photosite contains a photodiode, a capacitor, and up to four transistors. The photodiode is the primary light-sensing component in the imaging system and is based on a reverse-biased *p–n* junction for capturing photogenerated electrons. The working principle of each photosite can be simply described as the following: according to quantum mechanics, the

1.3 Using the Smartphone Camera in Experiments

In this book, the smartphone camera is central to the experiments as a detector in several different contexts. To apply the smartphone camera to scientific experiments, there are several fundamental assumptions:

1. The sensor's response to light intensity is linear: either the RGB values or the grayscale value is proportional to the light intensity provided that the photosite is not saturated.
2. All of the photosites in the sensor array are identical.
3. The spectral response of the sensors in the visible wavelength range is flat.
4. There is no image distortion.
5. The adaptive optical system can be treated as a single converging lens that can form a real image on the sensor array. The autofocus feature of the camera can adjust the effective focal length of the optical system so that the effective image distance of the camera is fixed; i.e., the distance between the sensor array surface and the effective lens is a constant for any image taken.
6. A scaling factor can be defined to convert the pixel length in a smartphone image to a real length.

The following precautions should also be taken during the experiments:

1. Avoid using the camera's "auto" photography feature because it may automatically change the exposure time during consecutive image acquisition.
2. Avoid using flash photography during image acquisition.
3. Avoid high intensity of light flux because it will saturate the photosite(s).
4. Avoid using images that are very small (i.e., only a few pixels in size) for length calibration, wavelength calibration, or image identification.
5. Maintain a consistent smartphone orientation when taking images. In most smartphones, images taken with a vertically oriented smartphone will have different pixel dimensions than images taken with a horizontally oriented smartphone.
6. If a multi-camera system is used, select the standard wide-angle camera for experimentation.

References

[1] N. Islam and R. Want, "Smartphones: past, present, and future," *IEEE Pervasive Comput*. **13**(4), 89–92 (2014).
[2] N. Ai, Y. Lu, and J. Deogun, "The smart phones of tomorrow," *SIGBED Rev*. **5**(1), Article 16 (2008).

Chapter 2
Experimental Data Analysis

2.1 Experiments and Measurement Error

2.1.1 General physics experimental procedure

Scientific experiments are used to evaluate a hypothesis or to measure a certain scientific quantity. They are crucial in advancing modern sciences and technologies. In particular, physics experiments are usually employed to establish a quantitative relationship among different physical parameters (e.g., the Cavendish experiment for measuring the force of gravity between masses, the measurement of electrostatic force as a function of test charge, etc.), to prove or confirm a particular theoretical prediction or hypothesis (e.g., general relativity, the existence of black holes, etc.), or to measure important physical constants (e.g., the speed of light in vacuum, the charge of an electron, Planck's constant, etc.). In the 400 years of modern science (since Galileo Galilei, 1564–1642), rigorous guiding principles have been adopted for scientific experiments. In particular, a physics experiment should adhere to at least the following steps.

Step 1: The purpose of an experiment. The purpose of an experiment could be to measure a specific parameter, to evaluate a relationship/hypothesis, or to establish a correlation. For example, to obtain the value of g, the acceleration of gravity, an experiment should be designed with the purpose of performing such a measurement.

Step 2: The design of an experiment. Based on our knowledge of introductory physics (or high school physics), there are various methods for measuring the value of g, such as the investigation of a free-falling solid ball, the sliding of a block on a frictionless slope (or air track), or the measurement of the period of a pendulum. Among the three methods suggested, the pendulum method is quite reliable and simple because the period T of the oscillation of a pendulum only depends on the length l of the pendulum (see Fig. 2.1):

$$T = 2\pi\sqrt{l/g} \tag{2.1}$$

or

$$\sigma_z = \sqrt{\left(\frac{\partial f}{\partial x}\sigma_x\right)^2 + \left(\frac{\partial f}{\partial y}\sigma_y\right)^2 + \ldots}. \tag{2.6}$$

For a two-variable function $z = f(x, y)$, with measured $x \pm \sigma_x$ and $y \pm \sigma_y$,

$$\text{if } z = x + y, \text{ or } x - y, \sigma_z = \sqrt{\sigma_x^2 + \sigma_y^2}; \tag{2.7}$$

$$\text{if } z = xy, \text{ or } x/y, \frac{\sigma_z}{z} = \sqrt{\frac{\sigma_x^2}{x^2} + \frac{\sigma_y^2}{y^2}}. \tag{2.8}$$

$$\text{Thus, for Eq. 2.2, } \sigma_g = 4\pi^2\sqrt{\left(\frac{\sigma_l}{T^2}\right)^2 + \left(\frac{2l\sigma_T}{T^3}\right)^2}. \tag{2.9}$$

As an example, if the measurements give $l = 1.00 \pm 0.01$ m and $T = 2.0 \pm 0.05$ s in a particular pendulum experiment, then σ_g is calculated to be 0.4 m/s^2 according to Eq. 2.9. Thus, the reported g value for this measurement is $g = 9.7 \pm 0.4$ m/s^2.

2.2 Numerical/Parameter Estimation

2.2.1 Estimation of a direct measurement

Due to errors and repeated measurements, it is important to know how to estimate a directly measured quantity. If random errors dominate the measurements, the following equations can be used to numerically estimate the mean μ and the standard deviation σ:

$$\mu = \bar{x} = \frac{1}{N}\sum_{j=1}^{N} x_j, \tag{2.10}$$

$$\sigma = \sqrt{\frac{1}{N-1}\sum_{j=1}^{N}(x_j - \bar{x})^2}, \tag{2.11}$$

where N is the number of measurements and x_j is the value of the jth measurement; thus, the reported measurement value should be $x_{report} = \mu \pm \sigma$ (unit).

Because random noise is intrinsic to any instrument or measurement, it is expected that even for the jth measurement, the reported x_j value should also

Equations 2.20–2.23 give the results for the least-squares fitting for a linear function. In many cases, the relationships measured in an experiment may not be linear. In these cases, nonlinear least-squares fitting is needed. To obtain the best-fitting parameters for nonlinear functions, two different strategies can be used: the model function can be converted into a linear function, so that the above linear least-squares fitting equations can be used for the converted function to determine the desired parameters; or, if the function cannot be converted to a linear function, some special methods can be used to estimate the optimized parameters (see Johnson [3]). The latter strategy involves mathematical knowledge beyond the undergraduate level; if interested, refer to [3] or other related literature. The first strategy depends on the detailed expression of the nonlinear function. For example, if a power function is used to model the y–x relationship,

$$y = ax^b \ (a > 0), \tag{2.24}$$

where a and b are the fitting parameters; this power function can then be converted into a linear function by letting $X = \ln x$ and $Y = \ln y$, so that Eq. 2.24 becomes

$$Y = \ln a + bX. \tag{2.25}$$

Therefore, a linear least-squares fitting can be used for the X–Y relationship in Eq. 2.25 to determine the parameters $\ln a$ and b. Many other nonlinear functions can also be converted to a linear function. Table 2.1 lists some representative functions and the corresponding conversions.

Table 2.1 Some representative nonlinear functions and their conversions to linear functions.

Orginal function	Conversion	Equivalent linear function
$y = ae^{bx}$ $(a > 0)$	$X = x$ and $Y = \ln y$	$Y = \ln a + bX$
$y = ae^{bx^2}$ $(a > 0)$	$X = x^2$ and $Y = \ln y$	$Y = \ln a + bX$
$y = ae^{b/x}$ $(a > 0)$	$X = 1/x$ and $Y = \ln y$	$Y = \ln a + bX$
$y = ax^b + c$	$X = \ln x$ and $Y = \ln (y - c)$	$Y = \ln a + bX$
$y = \frac{x}{ax+b} + c\,(a, c > 0)$	$X = 1/x$ and $Y = 1/(y - c)$	$Y = a + bX$
$y = \frac{1}{ax+b}\,(a > 0)$	$X = x$ and $Y = 1/y$	$Y = b + aX$

2.3 Model Testing

Another important issue regarding experimental data analysis is how to assess the model used to fit the experimental data, i.e., whether the fitting function used is a good model to fit the experimental data. From the previous section, with the experimental data and a proposed model (relationship), a least-squares method can be used to give the best estimation for the corresponding

Chapter 3
Law of Reflection

3.1 Introduction

The law of reflection is a principle that describes a ray of light reflecting off a smooth surface. It states that when a ray strikes the surface, the angle of reflection θ_r is equal to the angle of incidence θ_1, i.e., $\theta_1 = \theta_r$, as shown in Fig. 3.1. Notice that the angles θ_r and θ_1 are defined with respect to the surface normal.

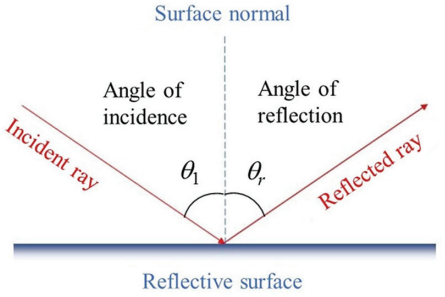

Figure 3.1 The law of reflection.

3.2 Smartphone Experiment (Alec Cook and Ryan Pappafotis, 2015)

3.2.1 General strategy

In this experiment, the smartphone acts as an imaging device that records the incident and the reflected laser rays into and out of a mirror's surface. After capturing photos at various laser incident angles, both the angle of incidence θ_1 and the angle of reflection θ_r can be extracted from the image, and a plot of θ_r versus θ_1 can be generated with a slope equal or close to 1, which demonstrates the law of reflection.

Chapter 4
Law of Refraction

4.1 Introduction

The law of refraction is the principle describing a ray of light that is incident from one optical medium to another optical medium at a smooth interface. The angle of incidence (θ_1) and the angle of refraction (θ_2) as shown in Fig. 4.1 obey Snell's law, $n_1 \sin \theta_1 = n_2 \sin \theta_2$, which is determined by the refractive indices n_1 and n_2 of the two media. Notice that each angle is defined with respect to the surface normal.

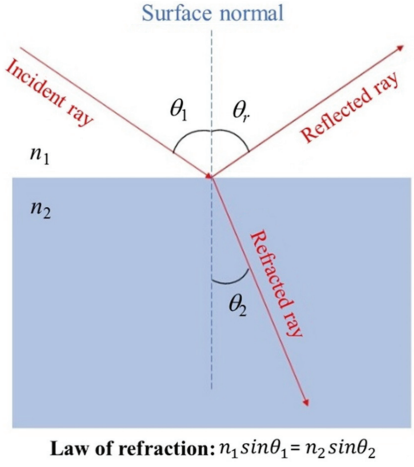

Figure 4.1 The law of refraction.

4.2 Smartphone Experiment (Alec Cook and Ryan Pappafotis, 2015)

4.2.1 General strategy

In this experiment, the smartphone acts as an imaging device for recording the incident and refracted laser beams at the air–glass interface. After capturing images at various incident angles, the angle of incidence θ_1 and the angle of

Chapter 6
Linear Polarization

6.1 Introduction

Light is a transverse electromagnetic (EM) wave in which the oscillation directions of the electric field and the magnetic field are perpendicular to its propagation direction. Linearly polarized light is an EM wave with a constant orientation direction for the oscillating electric field, wherein the orientation of its electric field defines the direction of the polarization. As shown in Fig. 6.1, a linearly polarized light with a polarization along the x direction and a propagation direction along the z axis can be written as

$$\vec{E}_x = \hat{x}E_{x0}\cos(k_\lambda z - \omega t), \tag{6.1}$$

where E_{x0} is the amplitude of the electric field, $\hat{x}$ is the unit vector along the x axis, and k_λ and ω are the wave number and angular frequency of the EM wave, respectively. The output of light sources such as the Sun, flashlights, and household lamps, are not linearly polarized, whereas a laser's output, on the other hand, is linearly or partially polarized. One can use a polarizer to change unpolarized light into linearly polarized light. Every polarizer has a polarization axis identified by the manufacturer. An ideal polarizer only allows the component of the electric field parallel to its polarization axis to be fully transmitted. For instance, Fig. 6.1 depicts a polarizer whose polarization axis forms an angle α with respect to the x axis. If a linearly polarized light propagates through the polarizer, the electric field $\vec{E}_p$ transmitted through the polarizer is expressed as

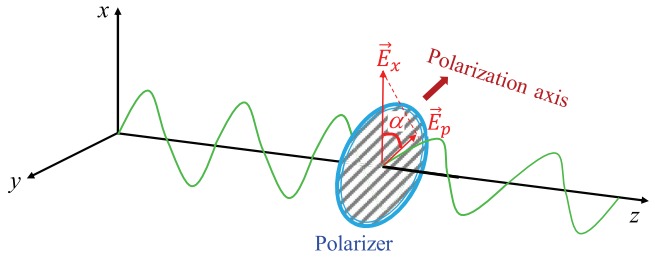

Figure 6.1 Linearly polarized light passing through a polarizer.

$$\vec{E}_p = E_{x0}\cos\alpha(\hat{x}\cos\alpha - \hat{y}\sin\alpha)\cos(k_\lambda z - \omega t). \tag{6.2}$$

Thus, the intensity I_p of the light passing through a linear polarizer can be written as

$$I_p(\alpha) = I_0\cos^2\alpha, \tag{6.3}$$

where $I_0 = \frac{1}{2}c\varepsilon_0 E_{x0}^2$ is the intensity of the incident light. Equation 6.3 is known as Malus's law, and it describes the basic properties of a linearly polarized light transmitted through a polarizer.

6.2 Smartphone Experiment (Sungjae Cho and Aojie Xue, 2019)

6.2.1 General strategy

To demonstrate Malus's law, two polarizers are used to measure the change of light intensity as a function of the relative angle of the polarization axes. The smartphone camera is used as a light intensity detector. One should ensure that the intensity of light does not saturate the camera's highest intensity limit.

6.2.2 Materials

1. A smartphone
2. A laser pointer
3. A laser pointer holder
4. Two sheet polarizers
5. Two polarizer holders
6. A printed protractor
7. A smartphone holder

6.2.3 Experimental setup

The experimental setup is shown in Fig. 6.2 (more experimental setups can be found in Chapter 21). Depending on the dimension of the laser pointer, polarizer sheets, and the smartphone, three simple holders, as shown in Fig. 6.2, are designed and 3D printed. Both the holders for the laser pointer and the smartphone are U-shaped slots that allow items to fit snugly within them. A hole is designed in the smartphone holder to accommodate the smartphone camera. The holders for the polarizer sheets are rectangular frames with rectangular openings. The polarizer sheets are taped to these rectangular frames so that they can be removed and reattached conveniently. The orientation of one polarizer is changed using a protractor. In this setup, one should ensure that the center of the laser pointer, the hole in the smartphone holder, and the center of the rectangular opening in the polarizer holder are aligned and at the same height.

Chapter 10
Thin Film Interference

10.1 Introduction

When light shines onto a thin film sandwiched between two dielectric media, an interference pattern can be formed due to the reflection at these two interfaces when the two reflected beams merge together at a large distance from them. For example, the rainbow colors in soap bubbles are a result of thin film interference. As shown in Fig. 10.1(a), a thin film with a thickness d_{film} and a refractive index n_2 is sandwiched between two media with refractive indices n_1 and n_3, respectively. The light with an incident angle θ_1 at the interface of media n_1 and n_2 reflects and transmits at the location A. This reflected beam is denoted as Beam 1. The transmitted beam reflects at the interface of media n_2 and n_3 at the location B and emerges at location C of the n_1 and n_2 interface. This emerging beam is denoted as Beam 2. Both Beam 1 and Beam 2 are parallel to each other and can interfere with each other at a large distance away from the thin film surface. Because this interference occurs far away, a lens is needed to observe the fringes. Clearly, Beam 2 propagates an extra distance when both beams meet at location P. Based on the geometric relationship between Beam 1 and Beam 2, the optical path length difference Λ between the two beams is

$$\Lambda = 2n_2 d_{film} \cos\theta_2. \tag{10.1}$$

The bright interference fringe will form when $\Lambda = m\lambda$, where m is an integer and λ is the wavelength of the light in vacuum (or air). Thus, the corresponding refractive angle θ_2^m is

$$d_{film} \cos\theta_2^m = \frac{m\lambda}{2n_2}. \tag{10.2}$$

The refractive angle θ_2^m is closely linked with the incident angle θ_1^m by Snell's law. Therefore, to form a thin film interference pattern, the incident light

Chapter 14
Optical Rangefinder Based on Gaussian Beam of Lasers

14.1 Introduction

Rangefinders have a variety of applications, from robotics to airborne topographic mapping. Most rangefinders in the market utilize complicated electronic and optical systems. For example, as shown in Fig. 14.1, an electro-optical rangefinder makes use of the transit time of an electromagnetic signal reflected from the target to estimate the distance between itself and a target. Other types of rangefinders, ultrasonic sensors, radar, and sonar, operate on similar principles. In fact, an optical rangefinder can also be designed based on the Gaussian beam property of a laser.

The spatial distribution of the intensity I of a single-mode (known as the TEM_{00} mode) laser beam as a function of the radial distance r from the beam axis follows a Gaussian profile,

$$I(r) = I_0 e^{-2r^2/w^2}, \tag{14.1}$$

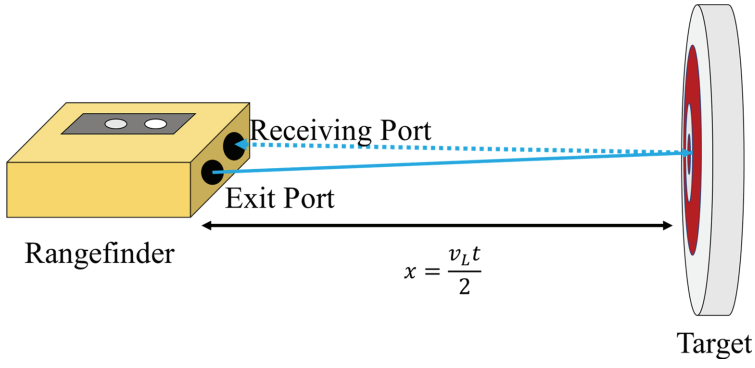

Figure 14.1 Electro-optical rangefinder: a laser beam travels at speed v_L from the exit port, reflects from the target, and enters the receiving port after time t.

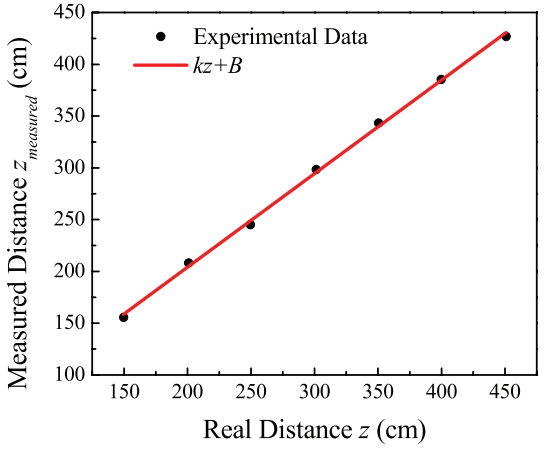

Figure 14.5 The plot of the extracted distance $z_{measured}$ from the rangefinder versus the actual distance z. The data are fit with a linear function $z_{measured} = kz + B$. The extracted fit parameters are $k = 0.90 \pm 0.05$ and $B = 23 \pm 4$ cm.

calibration process, a series of photos of the two laser spots on a movable screen is taken when the screen is placed at different distances z from the rangefinder. The photos of the two laser spots on the screen are then analyzed by ImageJ software, the actual laser spot diameter $2w$ in each photo is determined, and the distance $z_{measured}$ is extracted using Eq. 14.4. The actual distance z is also measured with a tape measure. Figure 14.5 plots $z_{measured}$ versus z obtained in the experiment. Evidently, they follow a linear relationship, and the least-squares fitting gives a slope of 0.90 ± 0.05.

14.3 Smartphone Experiment II: Estimating the Beam Waist Parameter with a Single Laser (Joo Sung and Connor Skehan, 2015)

14.3.1 General strategy

In this single-laser optical rangefinder setup, the smartphone is used to take photos of the laser beam projection on a target from various distances. The images are used to calibrate a distance from the rangefinder to the target.

14.3.2 Materials

1. A smartphone
2. A red laser (650 nm)
3. LEGO®-constructed laser holder
4. A piece of white paper
5. A ruler
6. A cardboard backdrop

Chapter 17
Dispersion

17.1 Introduction

According to Snell's law, a light ray will bend when traveling from one medium into another because light travels at different speeds in these two media. Within a given medium, different colors of light also travel at different speeds because the refractive index n depends on the wavelength λ of light; i.e., n is a function of λ. In most optical media, a longer wavelength of light corresponds to a smaller refractive index. This phenomenon is called *dispersion* and was demonstrated by Newton's prism experiment in 1666, in which a white light incident on a glass prism generates a broad rainbow-colored light beam, as shown in Fig. 17.1. For glass or other transparent media, the dispersion relationship can be expressed by the Sellmeier equation [1],

$$n^2 = A + B/\left(1 - \frac{C}{\lambda^2}\right) + D/\left(1 - \frac{CE}{\lambda^2}\right), \tag{17.1}$$

where λ is the wavelength and A, B, C, D, and E are called the Sellmeier coefficients.

The refractive index n of a medium can be determined using the angle of minimum deviation through a prism made of the same medium. As shown in Fig. 17.2, when a light beam (Beam 1) is incident on an isosceles triangular prism with a vertex angle β_v and refractive index n, it refracts into the prism

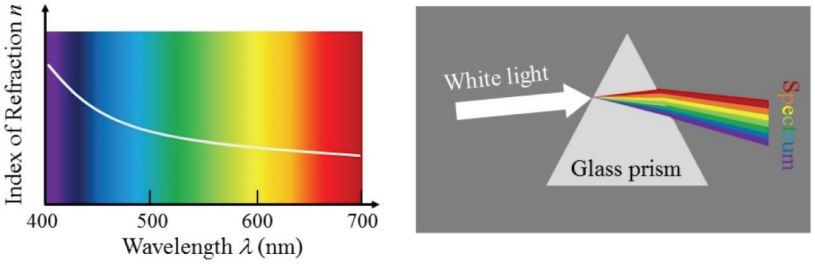

Figure 17.1 Dispersion of a medium. (Left) Refractive index n of a medium as a function of wavelength λ. (Right) Newton's prism experiment.

Chapter 21
Example Course Instructions for Smartphone-based Optical Labs

Below are example lab instructions given in the Introduction to Modern Optics class at the University of Georgia in the fall of 2020. At the beginning of the class, the students were instructed to learn the basics of the Python™ programming language by working through a Python tutorial on error analysis and data fitting. The labs followed this training. Detailed lab instructions are given below.

21.1 General Lab Instructions

21.1.1 Important notices for students

1. DO NOT shine the laser directly to anyone's eyes.
2. DO NOT directly touch the surfaces of lab materials with bare fingers where light will interact.
3. If you observe dust or fingerprints on the surfaces of materials, use a lens cloth to clean them. DO NOT attempt to blow on them with your mouth.

21.1.2 Lab materials

The following packed lab materials (all purchased from Amazon) are provided to the students (see Fig. 21.1):

1. Two AA batteries (~$18 for a 24-count pack)
2. A battery case (3 V) with switch (~$10 for 8 cases)
3. A laser diode (3 V, 650 nm, 5 mW) (~$6.50 for 10 pieces)
4. Two polarizer sheets (~$13 for an A5 size, cut into 1 cm × 3 cm pieces with the polarization direction along the short side)
5. One 1000 line/mm grating (~$12 for 25 pieces)

polarizer is along the short edge (depending on the cut on the polarizer sheet; this must be confirmed by the instructor).
   b. Measure both the reflected and transmitted intensity versus the incident angle θ_1. Students are encouraged to repeat each θ_1-related intensity measurement at least five times.
   c. Use the Fresnel equation for reflection (Eq. 7.1 in Chapter 7) to fit the reflection data and extract the refractive index n_2 for glass.
   d. Derive an equation based on the Fresnel equation for transmission (hint: there are two interfaces for transmission, the air–glass and glass–air interfaces), use it to fit the obtained transmission data, and obtain n_2.
2. Determine the Brewster angle at the air–glass interface (see Chapter 8):
   a. Calculate the expected Brewster angle based on the refractive index obtained from the first lab.
   b. Change the incident polarized light into p-polarization.
   c. Measure the reflection at the air–glass interface with the p-polarized light in the neighborhood of the estimated Brewster angle ($\pm$5 deg) with a fine adjustment of the incident angle (say, an increment of 1 or 0.5 deg).
   d. Determine the Brewster angle with repeated measurements.
3. Write and submit a lab report manuscript based on these two experiments.

21.3.3 Additional labs

The following labs can also be carried out using the constructed lab setup, and students can add the results to their lab report:

1. Test the Fresnel equation for other materials, such as water, oil, acrylic sheets, or other plastic sheets.
2. Determine the refractive index of these materials using the Brewster angle.

21.4 Interference Labs

21.4.1 Required lab materials

Unfortunately, the laser beam from the laser diode is not coherent enough for the planned labs, so students use a He–Ne laser in the lab.

1. A smartphone
2. A He–Ne laser
3. Three glass slides
4. Multiple small-cut strips of printer paper
5. Two lenses

Yiping Zhao is a Distinguished Research Professor at the Department of Physics and Astronomy at the University of Georgia, where he has taught undergraduate physics courses and conducted nanotechnology-based research since 2002. He obtained his Ph.D. in Physics at Rensselaer Polytechnic Institute in 1999. He is a Fellow of SPIE and the American Vacuum Society (AVS). Professor Zhao's research interests are nanostructure and thin film fabrication and characterization, plasmonics and metamaterials, chemical and biological sensors, nanophotocatalysts, nanomotors, and nanotechnology for disease treatment.

Yoong Sheng Phang is a Ph.D. student and National Science Foundation (NSF) Graduate Research Fellow in the Department of Physics at Harvard University. He received his B.S. degrees in Physics and Mathematics in 2022 at the University of Georgia, where he conducted undergraduate research on magnetic nanomotors and smartphone optics in Professor Zhao's lab. His Ph.D. research is focused on experimental investigations of quantum materials.